



The following Communications have been judged by at least two referees to be “very important papers” and will be published online at www.angewandte.org soon:

M. Mascal*, E. B. Nikitin

Direct, High-Yield Conversion of Cellulose into Biofuel

P. García-Álvarez, D. V. Graham, E. Hevia, A. R. Kennedy, J. Klett, R. E. Mulvey*, C. T. O'Hara, S. Weatherstone

Unmasking Representative Structures of TMP-Active Hauser and Turbo Hauser Bases

T. Robert, J. Velder, H.-G. Schmalz*

Enantioselective Copper-Catalyzed 1,4-Addition of Grignard Reagents to Cyclohexenone Using Taddol-Derived Phosphine–Phosphite Ligands and 2-Methyl-THF as a Solvent

A. D. Shaller, W. Wang, H. Gan, A. D. Q. Li*

Tunable Molecular Assembly Codes Direct Reaction Pathways

K. C. Nicolaou*, Y.-P. Sun, X.-S. Peng, D. Polet, D. Y.-K. Chen*

Total Synthesis of (+)-Cortistatin A

D. Staack, A. Fridman, A. Gutsol, Y. Gogotsi*, G. Friedman*

Nanoscale Corona Discharge in Liquids Enabling Nanosecond Optical Emission Spectroscopy

C. Hawner, K. Li, V. Cirriez, A. Alexakis*

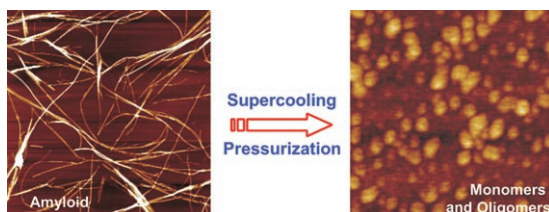
Copper-Catalyzed Asymmetric Conjugate Addition of Aryl Aluminum Reagents to Trisubstituted Enones: Construction of Aryl-Substituted Quaternary Centers

Asymmetric Organic Synthesis with Enzymes

Vicente Gotor, Ignacio Alfonso, Eduardo García-Urdiales

Books

reviewed by P. Berglund — 6514



Cold denaturation (including supercooling) and pressure perturbation are able to dissolve protein aggregates and, in some cases, amyloid fibrils (see picture). These studies provide additional details on the

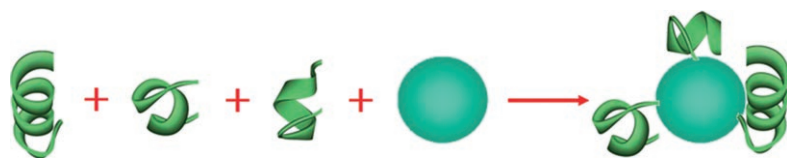
polymorphic forms of amyloid structures and their precursors as well as the transformation processes between polymorphic states.

Highlights

Amyloid Dissociation

R. Mishra, R. Winter* — 6518–6521

Cold- and Pressure-Induced Dissociation of Protein Aggregates and Amyloid Fibrils



When Protein met Metal: The ability of metal ions to coordinate the assembly of specific supramolecular protein complexes (see schematic representation)

enables the development of experimental and bioinformatic techniques for probing protein–protein interactions.

Protein Structures

K. Kerman, H.-B. Kraatz* — 6522–6524

Metals Coordinate Protein–Protein Interactions

Minireviews

Metal–Metal Complexes

E. Carmona,* A. Galindo — 6526–6536

Direct Bonds Between Metal Atoms: Zn, Cd, and Hg Compounds with Metal–Metal Bonds



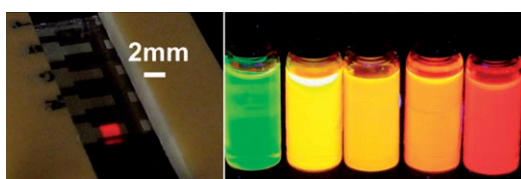
Sticking together: In the past few years, several compounds with stable Zn–Zn bonds have been reported, the existence of which was previously considered highly doubtful. Interest in this area was sparked by $[\text{Zn}_2(\eta^5\text{-C}_5\text{Me}_5)_2]$, in which the $[\text{Zn}–\text{Zn}]^{2+}$ unit is coordinated by two eclipsed C_5Me_5 ligands (see structure; Zn green, C gray). Homologous Cd and Hg species have been discovered as well.

Reviews

Nanoelectronics

A. L. Rogach, N. Gaponik, J. M. Lupton, C. Bertoni, D. E. Gallardo, S. Dunn, N. Li Pira, M. Paderi, P. Repetto, S. G. Romanov, C. O'Dwyer, C. M. Sotomayor Torres, A. Eychmüller* — 6538–6549

Light-Emitting Diodes with Semiconductor Nanocrystals



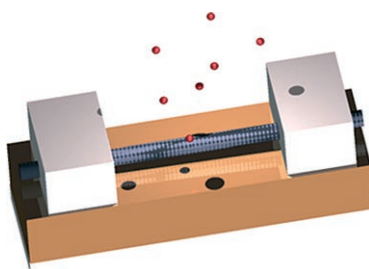
Small things bright and beautiful: research into light-emitting diodes (LEDs) made from semiconductor nanocrystals has advanced significantly in just one decade: external quantum efficiency has improved by over two orders of magnitude and highly saturated color emission

is now the norm (see picture; nanocrystalbased LED and size-dependent photoluminescence of CdTe nanocrystals). The nanocrystal devices have potential advantages over purely organic LEDs such as spectrally pure emission.

Nanotechnology

D. R. Kauffman, A. Star* — 6550–6570

Carbon Nanotube Gas and Vapor Sensors



Big things from small materials: The incorporation of carbon nanotubes (CNTs) into electronic devices has led to the development of extremely sensitive and compact chemical sensors (see the model of a transistor with a CNT between two electrodes). These sensors utilize the unique phenomena occurring at the surface of nanometer-sized structures for the detection of trace amounts of gas- and vapor-phase analytes.

For the USA and Canada:

ANGEWANDTE CHEMIE International Edition (ISSN 1433-7851) is published weekly by Wiley-VCH, PO Box 191161, 69451 Weinheim, Germany. Air freight and mailing in the USA by Publications Expediting Inc., 200

Meacham Ave., Elmont, NY 11003. Periodicals postage paid at Jamaica, NY 11431. US POSTMASTER: send address changes to *Angewandte Chemie*, Wiley-VCH, 111 River Street, Hoboken, NJ 07030. Annual subscription price for institutions: US\$ 7225/6568 (valid for print and

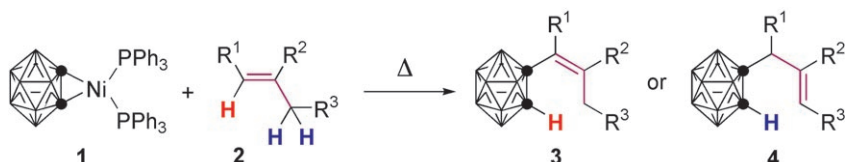
electronic / print or electronic delivery); for individuals who are personal members of a national chemical society prices are available on request. Postage and handling charges included. All prices are subject to local VAT/sales tax.

Communications

Coupling Reactions

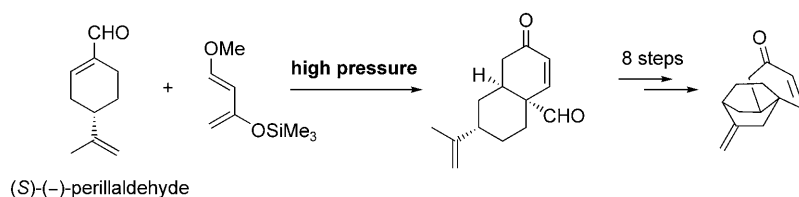
Z. Qiu, Z. Xie* — 6572–6575

Nickel-Mediated Coupling Reactions of Carboryne with Alkenes: A Synthetic Route to Alkenylcarboranes



Happily coupled: A nickel–carboryne complex **1** reacts with substituted styrenes **2** to afford alkenylcarboranes in moderate to very good yields with excellent regio- and stereoselectivity. Either the “Heck-type” (**3**) or the “ene-reaction-type”

product (**4**) could be isolated (see scheme). A reaction mechanism that involves alkene insertion followed by successive β-H elimination and reductive elimination steps is proposed.



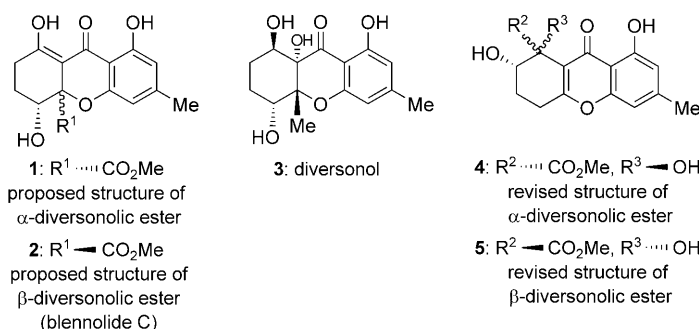
Bacteria under pressure! An efficient synthesis of the enantiopure tricyclic core of a recently discovered antibiotic, platencin, has been developed. This synthesis highlights a novel high-pressure

Diels–Alder reaction of the flavoring agent (S)-(-)-perillaldehyde and an efficient SmI_2 -mediated pinacol cyclization for the construction of the bicyclo[2.2.2]octane framework (see scheme).

Natural Product Synthesis

D. C. J. Waalboer, M. C. Schaapman, F. L. van Delft, F. P. J. T. Rutjes* — 6576–6578

High-Pressure Entry into Platencin



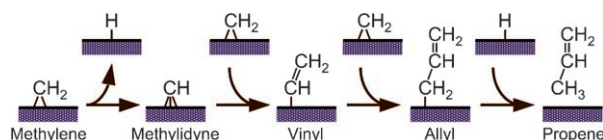
Expedient total syntheses of the originally proposed structures of the naturally occurring α- and β-diversonolic esters (**1**

and **2**) and diversonol (**3**) lead to the revision of the structures of **1** and **2** to **4** and **5**, respectively (see structures).

Natural Product Synthesis

K. C. Nicolaou,* A. Li — 6579–6582

Total Syntheses and Structural Revision of α- and β-Diversonolic Esters and Total Syntheses of Diversonol and Blennolide C



A four-step mechanism for thermal activation of methylene species on V(100) surfaces to generate propene is identified experimentally (see scheme). Dehydrogenation of methylene to methylidyne and coupling with another methylene group

gives a vinyl intermediate, which reacts with a methylene group to form an allyl species, which is finally hydrogenated to propene. This provides evidence for the possible role of vinyl intermediates in Fischer–Tropsch synthesis.

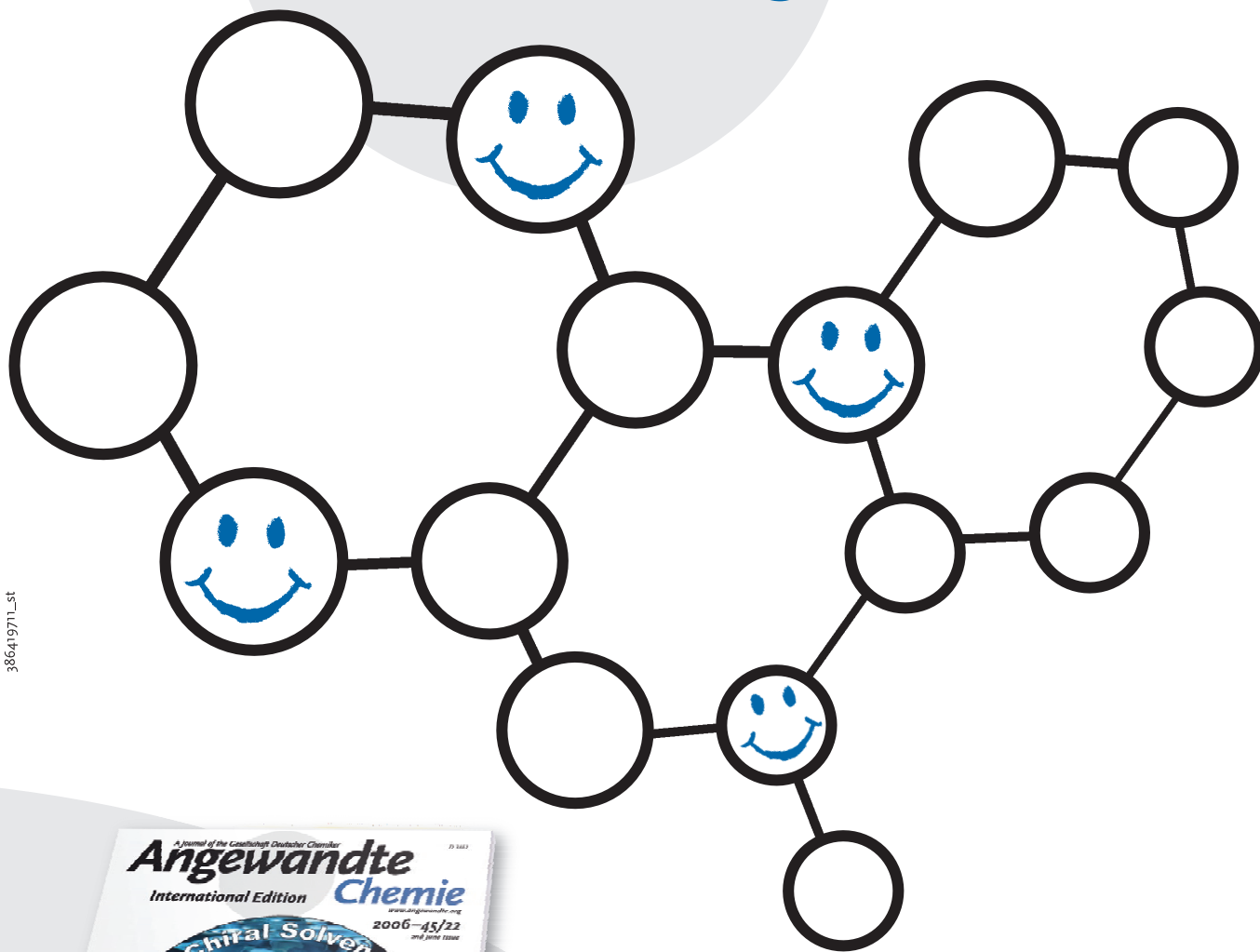
Surface Chemistry

M. Shen, F. Zaera* — 6583–6585

Hydrocarbon Chain Growth on V(100) Single-Crystal Surfaces via Vinyl Intermediates



Incredibly reader-friendly!



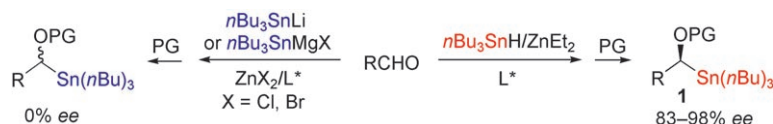
An aesthetically attractive cover picture that arouses curiosity, a well-presented and most informative graphical table of contents, and carefully selected articles that are professionally edited give *Angewandte Chemie* its distinctive character, which allows both easy browsing and further in-depth reading. Nearly 20 well-trained chemists, as well as eight further associates, work week in and week out to assemble reader-friendly issues and daily Early View articles online.



GESELLSCHAFT
DEUTSCHER CHEMIKER



service@wiley-vch.de
www.angewandte.org



Li and Mg are pesky: A catalytic asymmetric synthesis of α -(hydroxyalkyl)-tri-*n*-butylstannanes (**1**) in good to excellent yields and enantioselectivities was achieved (see scheme; PG = protecting group; L* = chiral ligand). Compound **1**

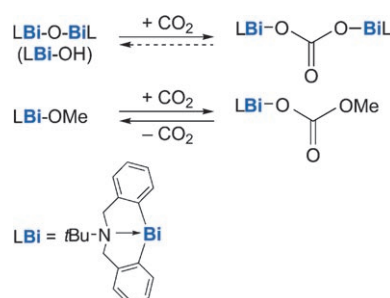
was isolated as an ester or thiocarbamate, and the reagent was prepared from equimolar amounts of *n*Bu₃SnH and Et₂Zn in dimethoxyethane. Conditions employing lithium or magnesium ions suppress enantioselectivity.

Synthetic Methods

A. He, J. R. Falck* _____ 6586–6589

Synthesis of Enantioenriched α -(Hydroxyalkyl)-tri-*n*-butylstannanes

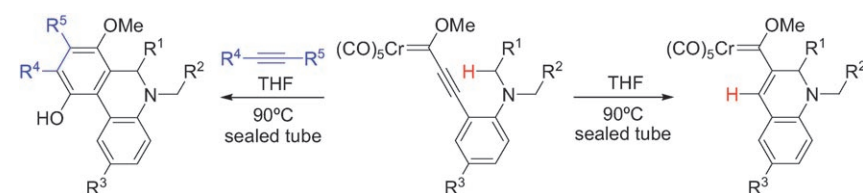
Keeping the lid on CO₂: Atmospheric CO₂ can be trapped irreversibly by hypervalent organobismuth oxide and hydroxide compounds, while an analogous alkoxide binds this greenhouse gas reversibly (see scheme). The hypervalent nature of the bismuth compounds is shown to play a decisive role in these reactions.



CO₂ Fixation

S.-F. Yin, J. Maruyama, T. Yamashita, S. Shimada* _____ 6590–6593

Efficient Fixation of Carbon Dioxide by Hypervalent Organobismuth Oxide, Hydroxide, and Alkoxide



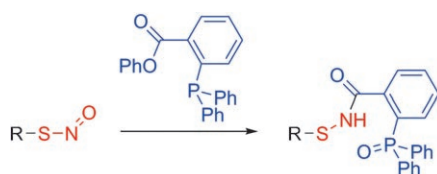
Trigger happy: A new cascade process initiated by an unprecedented [1,5]-hydride transfer/cyclization of *ortho*-amino phenyl alkynyl Fischer carbene complexes

leads to the formation of new 1,2-dihydroquinolinyl carbene complexes and 5,6-dihydrophenanthridine derivatives (see scheme).

Synthetic Methods

J. Barluenga,* M. Fañanás-Mastral, F. Aznar, C. Valdés _____ 6594–6597

[1,5]-Hydride Transfer/Cyclizations on Alkynyl Fischer Carbene Complexes: Synthesis of 1,2-Dihydroquinolinyl Carbene Complexes and Cascade Reactions



“Nitroso” knows: A process has been developed which converts unstable S-nitrosothiols into stable sulfenamide analogues (see scheme). Reductive ligation proceeds rapidly in mixed organic

solvent/water systems to give high yields. By applying this reaction, an efficient strategy for detecting S-nitrosylation in proteins and other biological systems is envisioned.

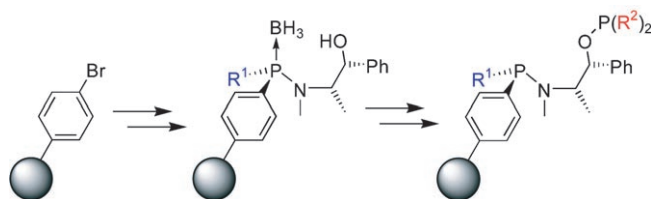
Nitrogen Oxides

H. Wang, M. Xian* _____ 6598–6601

Fast Reductive Ligation of S-Nitrosothiols

Immobilized Catalysts

R. den Heeten, B. H. G. Swennenhuis,
P. W. N. M. van Leeuwen, J. G. de Vries,
P. C. J. Kamer* 6602–6605

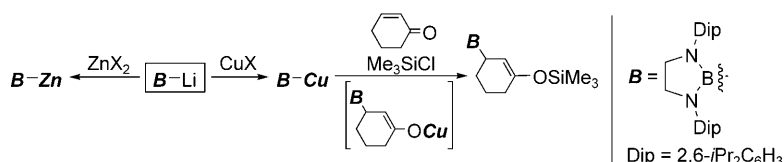


Bound to Ps: An efficient, rapid, parallel solid-phase synthesis of a series of resin-bound P-stereogenic aminophosphane–phosphinite and –phosphite ligands is

developed (see scheme). The ligands form active hydrogenation catalysts, displaying moderate to good enantioselectivities.

Boryl Anions

T. Kajiwara, T. Terabayashi, M. Yamashita,*
K. Nozaki* 6606–6610

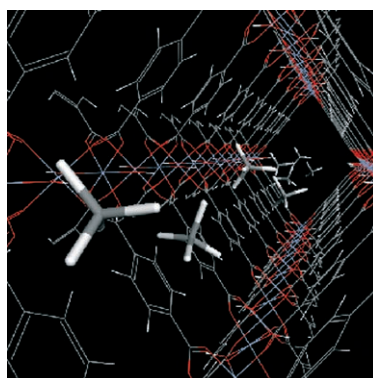


New borylcopper and borylzinc compounds were synthesized by transmetalation of boryllithium with metal halides. The 1,4-addition of lithium borylbromocuprate $[BCu(\mu^2-Br)Li(thf)_3]$ to 2-cyclo-

hexen-1-one as a boryl anion, followed by trapping of the resulting boron-substituted copper enolate with Me_3SiCl , afforded the γ -siloxyallylborane.

Diffusion in Porous Materials

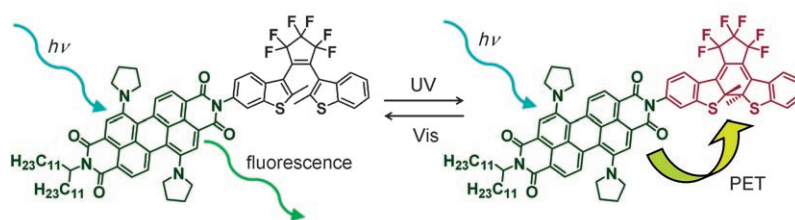
N. Rosenbach, Jr., H. Jobic,* A. Ghoufi,
F. Salles, G. Maurin,* S. Bourrelly,
P. L. Llewellyn, T. Devic, C. Serre,
G. Férey 6611–6615



Channel tunnel: Diffusion of methane in the metal–organic frameworks MIL-53(Cr) and MIL-47(V) was elucidated by quasi-elastic neutron scattering and molecular dynamics simulation, and 1D diffusion of CH_4 along the channels was found in both materials. The self-diffusivity of methane at low loading is very large, more than one order of magnitude higher than in zeolites. The picture shows CH_4 molecules in a MIL-53(Cr) channel.

Molecular Switches

M. Berberich, A.-M. Krause, M. Orlandi,
F. Scandola,* F. Würthner* 6616–6619



Flicking a switch: Photoinduced electron transfer (PET) occurs between the perylene and the closed (but not the open) form of the diarylethene unit in a prototype optical memory system based on a photochromic diarylethene-perylene bis-

imide dyad (see picture). This allows three different wavelengths to be used for the read, write, and erase steps without destructive readout occurring by photochromic cycloreversion.



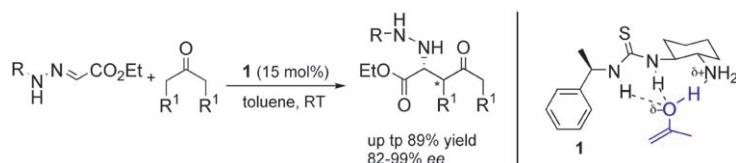
A versatile metal: Germanium was effectively used in a novel and efficient method for the Mannich-type reaction between α -bromoketones and simple *N*-alkyl imines (see scheme). Germanium(II) acts as a reducing agent, forming a nucleo-

phile for C–C bond formation. The Mannich adduct is effectively stabilized by the germanium center. Various *N*-alkylaldimines, including enolizable imines and formaldimines, can be used in this reaction system.

Synthetic Methods

S.-y. Tanaka, N. Tagashira, K. Chiba, M. Yasuda, A. Baba* — 6620–6623

Germanium(II)-Mediated Reductive Mannich-Type Reaction of α -Bromoketones to *N*-Alkylimines



A tale of two mechanisms—enol versus enamine: Chiral primary amine–thiourea **1** catalyzes highly enantioselective Mannich-type addition of unmodified ketones to *N*-benzoylhydrazones (see scheme). The reaction does not require preformed

enolate equivalents, and the computational data for the mechanism indicates a preference for **1**-complexed enol intermediates rather than enamine intermediates.

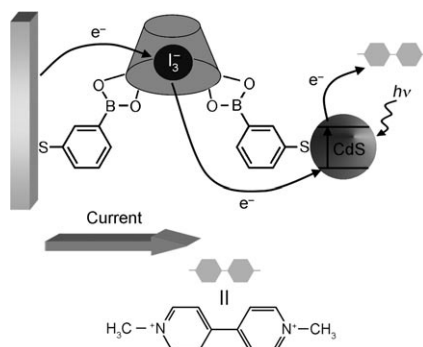
Organocatalysis

D. A. Yalalov, S. B. Tsogoeva,* T. E. Shubina, I. M. Martynova, T. Clark — 6624–6628

Evidence for an Enol Mechanism in a Highly Enantioselective Mannich-Type Reaction Catalyzed by Primary Amine–Thiourea



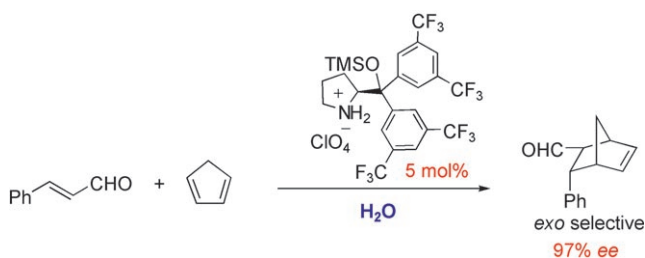
Changing direction: Gold electrodes have been linked to CdS nanoparticles through a β -cyclodextrin bridging unit (see scheme). The encapsulation of I_3^- or *N,N'*-dioctyl-4,4'-bipyridinium (octyl viologen) in the β -cyclodextrin cavities leads to enhanced photocurrents that are direction-controlled by the nature of the guest or by the addition of an inhibitor.



Photocurrent Generation

H. B. Yildiz, R. Tel-Vered, I. Willner* — 6629–6633

CdS Nanoparticles/ β -Cyclodextrin-Functionalized Electrodes for Enhanced Photoelectrochemistry



Water, water, everywhere: The title reaction predominantly affords the *exo* isomer with excellent enantioselectivity (see scheme; TMS = trimethylsilyl). The

synthesis can be carried out without organic solvents and provides the products by distillation. Water increases the rate and enantioselectivity of the reaction.

Synthetic Methods

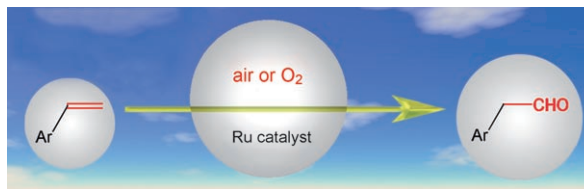
Y. Hayashi,* S. Samanta, H. Gotoh, H. Ishikawa — 6634–6637

Asymmetric Diels–Alder Reactions of α,β -Unsaturated Aldehydes Catalyzed by a Diarylprolinol Silyl Ether Salt in the Presence of Water



Aerobic Oxidation

G. Jiang, J. Chen, H.-Y. Thu, J.-S. Huang,
N. Zhu, C.-M. Che* — 6638 – 6642



Ruthenium Porphyrin-Catalyzed Aerobic Oxidation of Terminal Aryl Alkenes to Aldehydes by a Tandem Epoxidation–Isomerization Pathway

Catalytic oxidation of 1-alkenes to aldehydes by an epoxidation–isomerization pathway with air or dioxygen as terminal oxidant has been realized for bulky ruthenium(VI) porphyrin catalysts. For the new,

recyclable catalyst [Ru^{VI}(tmtp)₂O₂], product yields of up to 99% and total turnover numbers of up to 1144 were obtained.

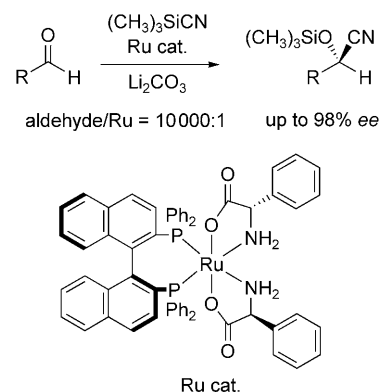
Asymmetric Catalysis

N. Kurono, K. Arai, M. Uemura,
T. Ohkuma* — 6643 – 6646



[Ru(phgly)₂(binap)]/Li₂CO₃: A Highly Active, Robust, and Enantioselective Catalyst for the Cyanosilylation of Aldehydes

The right combination: A series of aromatic, heteroaromatic, aliphatic, and α,β-unsaturated aldehydes can be converted into the desired silylated cyanohydrins by reaction with (CH₃)₃SiCN and a catalyst system consisting of the combination of a chiral ruthenium complex and Li₂CO₃ (see scheme). The reaction is highly enantioselective and affords the *R* products with up to 98% *ee* within 24 h at a substrate-to-catalyst ratio of 10000:1.

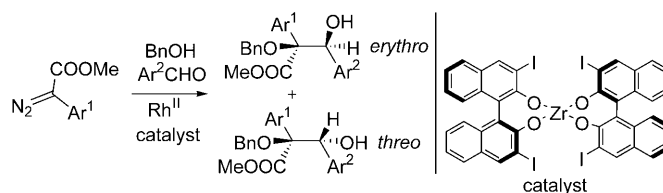


Multicomponent Reactions

X. Zhang, H. Huang, X. Guo, X. Guan,
L. Yang, W. Hu* — 6647 – 6649



Catalytic Enantioselective Trapping of an Alcoholic Oxonium Ylide with Aldehydes: Rh^{II}/Zr^{IV}-Co-Catalyzed Three-Component Reactions of Aryl Diazoacetates, Benzyl Alcohol, and Aldehydes



The right combination: A catalytic asymmetric multicomponent reaction has been developed in which two stereogenic carbon centers are constructed in a single step (see scheme; *erythro*/*threo* 90:10, up

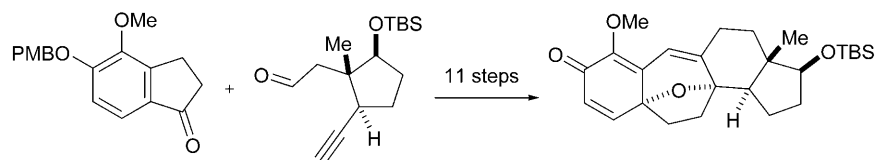
to 80% yield, 98% *ee*). This type of enantioselective three-component reaction generates α,β-dihydroxy acid derivatives in good yields and with excellent enantioselectivities. Bn = benzyl.

Natural Products

E. M. Simmons, A. R. Hardin, X. Guo,
R. Sarpong* — 6650 – 6653

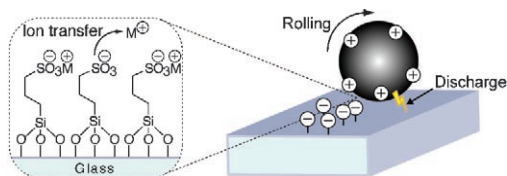


Rapid Construction of the Cortistatin Pentacyclic Core



Ring in cortistatin: The pentacyclic core of the cortistatin steroidal alkaloids has been readily assembled in eleven steps from simple building blocks (see scheme; PMB = *para*-methoxybenzyl,

TBS = *tert*-butyldimethylsilyl). An enyne cycloisomerization and an oxidative dearomatization/cyclization are the key ring-forming steps in this sequence.



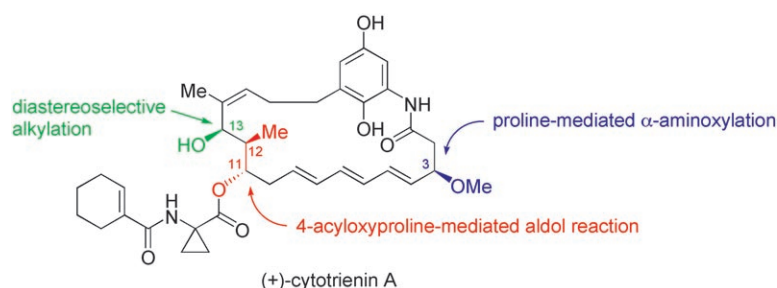
Episodic breakdown: The dynamics of contact electrification of a metal sphere rolling across an insulating plate are investigated. The data are consistent with

contact charging that involves the transfer of ions (see picture), interrupted by episodic discharge events that involve the dielectric breakdown of air.

Contact Electrification

S. W. Thomas, III, S. J. Vella,
G. K. Kaufman,
G. M. Whitesides* — 6654 – 6656

Patterns of Electrostatic Charge and Discharge in Contact Electrification



A star-studded lineup: (+)-Cytotrienin A was the target of an asymmetric total synthesis featuring an enantioselective aldol reaction, α -aminoxylation, deoxygenation, and a ring-closing metathesis to

form the 21-membered macrolactam. This first total synthesis confirms the relative and absolute configuration of the molecule.

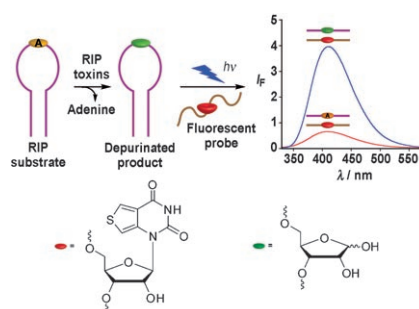
Natural Product Synthesis

Y. Hayashi,* M. Shoji, H. Ishikawa,
J. Yamaguchi, T. Tamura, H. Imai,
Y. Nishigaya, K. Takabe, H. Kakeya,
H. Osada — 6657 – 6660

The Asymmetric Total Synthesis of (+)-Cytotrienin A, an Ansamycin-Type Anticancer Drug



Lethal weapon: The presence of RNA abasic sites generated by ribosome-inactivating proteins (RIPs) such as ricin can be detected. RNA depurination by toxins is signaled by the enhanced emission intensity of synthetically modified emissive RNA constructs that are complementary to the α -sarcin/ricin loop (see picture). This method is more efficient and precise than the use of radiolabeled substrates.



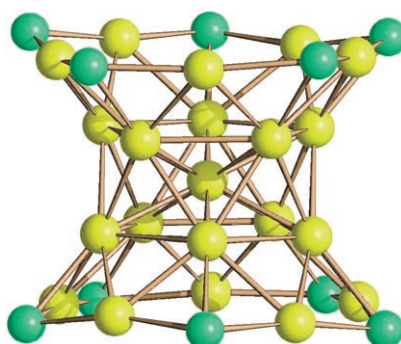
Fluorescent Probes

S. G. Srivatsan, N. J. Greco,
Y. Tor* — 6661 – 6665

A Highly Emissive Fluorescent Nucleoside that Signals the Activity of Toxic Ribosome-Inactivating Proteins



CO-vering gold: An organometallic approach to the synthesis of CO-protected Au–Fe nanoparticles led to solutions of colloids with hydrodynamic diameters between 4 and 300 nm, from which $[\text{Au}_{21}\{\text{Fe}(\text{CO})_4\}_{10}]^{5-}$ (picture: metal frame; Au yellow, Fe green), $[\text{Au}_{22}\{\text{Fe}(\text{CO})_4\}_{12}]^{6-}$, $[\text{Au}_{28}\{\text{Fe}(\text{CO})_3\}_4\{\text{Fe}(\text{CO})_4\}_{10}]^{8-}$, and $[\text{Au}_{34}\{\text{Fe}(\text{CO})_3\}_6\{\text{Fe}(\text{CO})_4\}_8]^{8-}$ were isolated. Their X-ray structures resemble those of gold–thiolate clusters.



Gold Nanoparticles

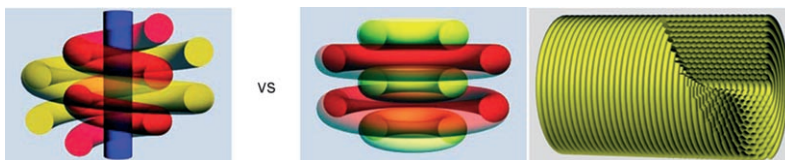
C. Femoni,* M. C. Iapalucci, G. Longoni,
C. Tiozzo, S. Zacchini — 6666 – 6669

An Organometallic Approach to Gold Nanoparticles: Synthesis and X-Ray Structure of CO-Protected $\text{Au}_{21}\text{Fe}_{10}$, $\text{Au}_{22}\text{Fe}_{12}$, $\text{Au}_{28}\text{Fe}_{14}$, and $\text{Au}_{34}\text{Fe}_{14}$ Clusters



Mesostructures

P. Yuan, N. Liu, L. Zhao, X. Zhou, L. Zhou,
G. J. Auchterlonie, X. Yao, J. Drennan,
G. Q. Lu, J. Zou,* C. Z. Yu* **6670–6673**



Solving Complex Concentric Circular
Mesostructures by Using Electron
Tomography

Inside knowledge: The true internal structure of a complex concentric circular hexagonal mesostructure has been solved for the first time by using electron tomography. This technique allows the mesostructure containing closed rings to be

differentiated from a closed helical mesostructure. The key step is the use of tomographic slices with a thickness of less than 1 nm so that the interior structure can be observed (see picture).

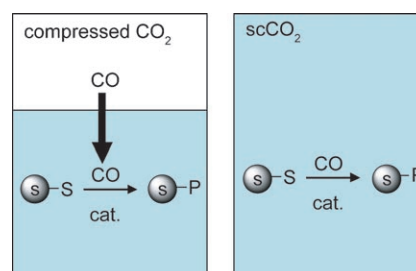
Solid-Phase Synthesis

A. Stobrawe, P. Makarczyk, C. Maillet,
J.-L. Muller, W. Leitner* **6674–6677**



Solid-Phase Organic Synthesis in the
Presence of Compressed Carbon Dioxide

Under pressure: The mass-transfer limitation in solid-phase organic synthesis with pressurized gaseous reagents is overcome by using carbon dioxide in the homogeneous supercritical state (right) for hydroformylation or under expanded-liquid conditions (left) for Pauson–Khand reactions. The use of standard high-pressure vessels and commercially available receptacles for the compartmentalization of substrates enables straightforward parallelization.

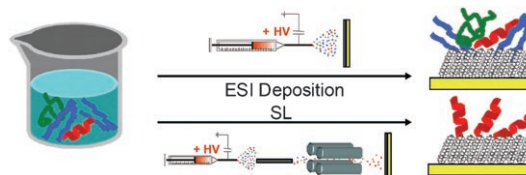


Peptide Arrays

P. Wang, J. Laskin* **6678–6680**



Helical Peptide Arrays on Self-Assembled
Monolayer Surfaces through Soft and
Reactive Landing of Mass-Selected Ions



Gently does it: Soft landing (SL) of mass-selected peptide ions can be used for preparation of conformation-specific peptide arrays on self-assembled monolayer surfaces. Deposition from solution

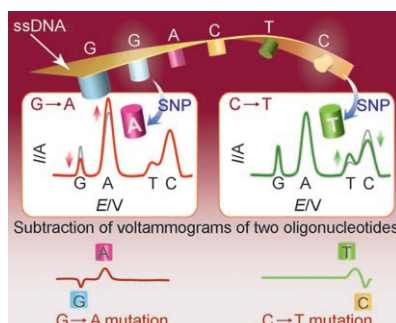
results in formation of a peptide layer dominated by the β -sheet structure, whereas with SL, a stable α -helical peptide layer on SAM surfaces is formed.

DNA Analysis

D. Kato, N. Sekioka, A. Ueda, R. Kurita,
S. Hirono, K. Suzuki,
O. Niwa* **6681–6684**

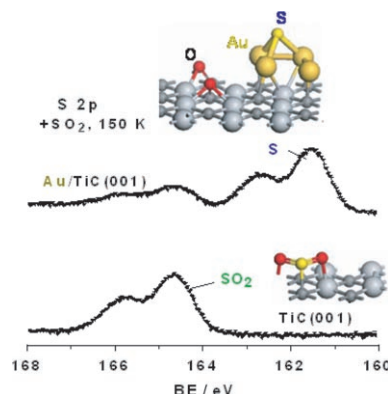


Nanohybrid Carbon Film for
Electrochemical Detection of SNPs
without Hybridization or Labeling



Base discrimination: A nanocarbon film electrode exhibits sufficiently high activity to obtain sharp, quantitative peaks for all the bases in an oligonucleotide. This property allows the label-free electrochemical analysis of single-nucleotide polymorphisms (SNPs) through the discrimination of single-base differences solely by using electrochemical oxidation (see picture; ssDNA = single-strand DNA).

Activating gold: High-resolution photoemission spectroscopy and DFT calculations were used to study the interaction of SO_2 with Au/TiC(001) surfaces. Both revealed molecular adsorption of SO_2 on TiC(001) but complete dissociation of the S–O bonds on Au/TiC(001) (see picture). Au/TiC(001) cleaves S–O bonds more efficiently than Au/TiO₂(110) or Au/MgO(100) and decomposes SO_2 at temperatures as low as 150 K.

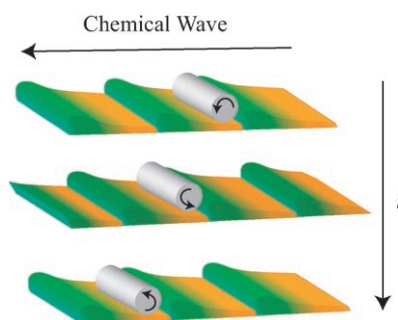


Surface Chemistry

J. A. Rodriguez,* P. Liu, F. Viñes, F. Illas, Y. Takahashi, K. Nakamura – **6685–6689**

Dissociation of SO_2 on Au/TiC(001): Effects of Au–C Interactions and Charge Polarization

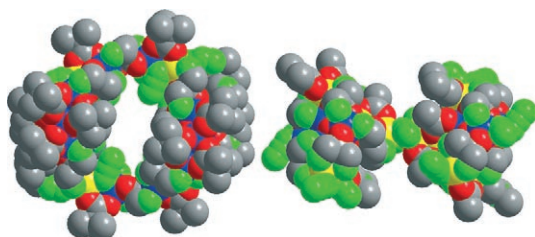
It's alive! A polymer gel has been developed that can generate a peristaltic motion without external stimuli. The motion is produced by dissipating the chemical energy of an oscillating reaction that occurs inside the gel. Although the gel is solely composed of a synthetic polymer, it shows independent motion as if it were alive. The motion of the gel can be harnessed to transport objects with millimeter dimensions (see picture).



Polymer Gels

S. Maeda,* Y. Hara, R. Yoshida, S. Hashimoto – **6690–6693**

Peristaltic Motion of Polymer Gels



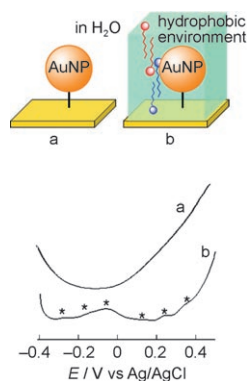
Double impact: The use of both azide and di-2-pyridylketone-derived ligands has provided new Mn₂₄ (left) and Mn₂₆ complexes (right) with loop and dumbbell structures that are made up of two covalently linked Mn₁₂ and Mn₁₃ units,

respectively. Both complexes are single-molecule magnets, and the Mn₂₆ complex displays the largest barrier for magnetization reversal in a Mn^{II/III} complex known to date. Mn^{II} yellow, Mn^{III} blue, O red, N green, C gray.

Cluster Compounds

T. C. Stamatatos, K. A. Abboud, W. Wernsdorfer, G. Christou* – **6694–6698**

Covalently Linked Dimers of Clusters: Loop- and Dumbbell-Shaped Mn₂₄ and Mn₂₆ Single-Molecule Magnets



The synergistic effect of the two surfactants hexyltrimethylammonium bromide and sodium dodecylbenzenesulfonate allows the redox peaks of Au nanoparticles (AuNPs) to be observed in the differential pulse voltammogram of an AuNP-modified Au electrode in aqueous solution (b), whereas in the presence of Et₄NClO₄ alone no significant peaks ascribable to AuNP redox processes appear due to the high dielectric constant of water (a).

Electron Transfer

M. Nakai, Y. Yamanoi, Y. Nishimori, T. Yonezawa, H. Nishihara* – **6699–6702**

Observation of Electrochemical Single-Electron-Transfer Events of Gold Nanoparticles in Aqueous Solution in the Presence of Both Ammonium and Sulfonate Surface-Active Agents

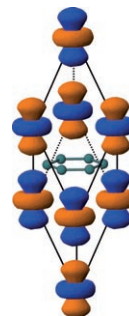


Electronic Structure

S. Deng,* A. Simon,
J. Köhler ————— 6703 – 6706

Calcium d States: Chemical Bonding of CaC_6

The Ca 3d state is a necessary and sufficient condition to produce an inter-layer band in CaC_6 according to model and first-principles studies, and this band cannot be considered to be a free-electron band. Involvement of the Ca 3d state in the chemical bonding and its tight-binding character explain the unusual Ca isotope effect in CaC_6 . The picture shows the orbital topology of one of the Fermi states of CaC_6 .

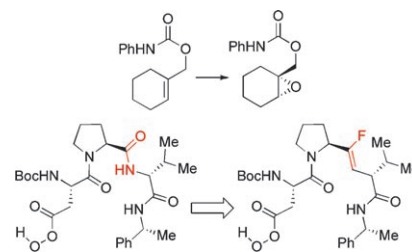


Asymmetric Epoxidation

C. E. Jakobsche, G. Peris,
S. J. Miller* ————— 6707 – 6711

Functional Analysis of an Aspartate-Based Epoxidation Catalyst with Amide-to-Alkene Peptidomimetic Catalyst Analogues

Subtle exchange: Replacement of an amide function with alkene or fluoroalkene groups provides a new class of epoxidation catalysts (see scheme). The structure-dependent catalytic behavior of these isosteric peptides provides mechanistic insights in their mode of action.

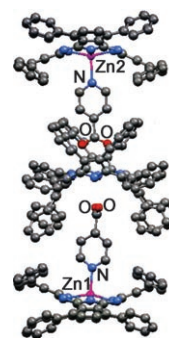


Supramolecular Chemistry

T. Kojima,* T. Honda, K. Ohkubo,
M. Shiro, T. Kusakawa, T. Fukuda,
N. Kobayashi,*
S. Fukuzumi* ————— 6712 – 6716

A Discrete Supramolecular Conglomerate Composed of Two Saddle-Distorted Zinc(II)-Phthalocyanine Complexes and a Doubly Protonated Porphyrin with Saddle Distortion Undergoing Efficient Photoinduced Electron Transfer

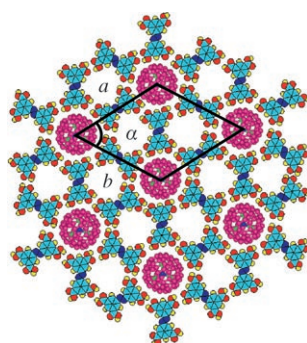
Blazing saddles: A supramolecular conglomerate is formed by intermolecular hydrogen bonding between two saddle-distorted Zn^{II} -phthalocyanine complexes coordinated by 4-pyridinecarboxylate and one doubly protonated saddle-distorted porphyrin dication. The assembly undergoes photoinduced intrasupramolecular electron transfer to generate an electron-transfer state with the lifetime of 667 ps.



Fullerenes

M. Li, K. Deng, S. B. Lei, Y. L. Yang,
T. S. Wang, Y. T. Shen, C. R. Wang,
Q. D. Zeng,* C. Wang* — 6717 – 6721

Site-Selective Fabrication of Two-Dimensional Fullerene Arrays by Using a Supramolecular Template at the Liquid-Solid Interface



A selective invitation: A 2D hydrogen-bonded porous network formed by an azobenzene derivative (NN4A) contains two different types of cavities and is shown to selectively accommodate fullerenes C_{60} and $\text{Sc}_3\text{N}@\text{C}_{80}$ (see picture). Highly ordered fullerene arrays are constructed at the liquid–solid interface of graphite by coadsorption of fullerenes and NN4A. While C_{60} occupies both types of cavity, C_{80} and $\text{Sc}_3\text{N}@\text{C}_{80}$ are only immobilized in one cavity type.

Supporting information is available on www.angewandte.org (see article for access details).



A video clip is available as Supporting Information on www.angewandte.org (see article for access details).

Sources

Product and Company Directory

You can start the entry for your company in "Sources" in any issue of *Angewandte Chemie*.

If you would like more information, please do not hesitate to contact us.

Wiley-VCH Verlag – Advertising Department

Tel.: ☎ 62 01 - 60 65 65

Fax: ☎ 62 01 - 60 65 50

E-Mail: MSchulz@wiley-vch.de

Service

Spotlights Angewandte's

Sister Journals _____ 6512 – 6513

Authors _____ 6722

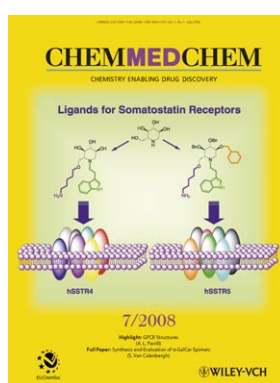
Keywords _____ 6724

Preview _____ 6725

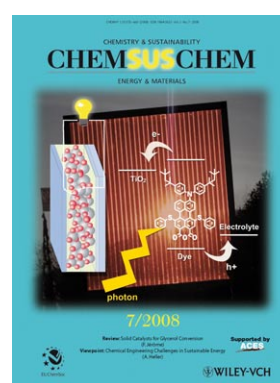
Check out these journals:



www.chemasianj.org



www.chemmedchem.org



www.chemsuschem.org